Biochimica et Biophysica Acta 1840 (2014) 1872–1881

Contents lists available at ScienceDirect

Biochimica et Biophysica Acta

journal homepage: www.elsevier.com/locate/bbagen

Role of glutamine-169 in the substrate recognition of human aminopeptidase B

Yuko Ogawa [a], Atsushi Ohnishi [a], Yoshikuni Goto [a], Yoshiki Sakuma [a], Jobu Watanabe [a], Akira Hattori [b], Masafumi Tsujimoto [a,*]

[a] Faculty of Pharmaceutical Sciences, Teikyo Heisei University, Nakano, Tokyo 164-8530, Japan
[b] Department of System Chemotherapy and Molecular Sciences, Graduate School of Pharmaceutical Sciences, Kyoto University, Kyoto 606-8501, Japan

ARTICLE INFO

Article history:
Received 24 September 2013
Received in revised form 26 December 2013
Accepted 2 January 2014
Available online 8 January 2014

Keywords:
Aminopeptidase
Catalytic pocket
Proteolytic processing
Site-directed mutagenesis
Substrate specificity

ABSTRACT

Background: Aminopeptidase B (EC 3.4.11.6, APB) preferentially hydrolyzes N-terminal basic amino acids of synthetic and peptide substrates. APB is involved in the production and maturation of peptide hormones and neurotransmitters such as miniglucagon, cholecystokinin and enkephalin by cleaving N-terminal basic amino acids in extended precursor proteins. Therefore, the specificity for basic amino acids is crucial for the biological function of APB.

Methods: Site-directed mutagenesis and molecular modeling of the S1 site were used to identify amino acid residues of the human APB responsible for the basic amino acid preference and enzymatic efficiency.

Results: Substitution of Gln169 with Asn caused a significant decrease in hydrolytic activity toward the fluorescent substrate Lys-4-methylcoumaryl-7-amide (MCA). Substantial retardation of enzyme activity was observed toward Arg-MCA and substitution with Glu caused complete loss of enzymatic activity of APB. Substitution with Asn led to an increase in IC_{50} values of inhibitors that interact with the catalytic pocket of APB. The EC_{50} value of chloride ion binding was also found to increase with the Asn mutant. Gln169 was required for maximal cleavage of the peptide substrates. Molecular modeling suggested that interaction of Gln169 with the N-terminal Arg residue of the substrate could be bridged by a chloride anion.

Conclusion: Gln169 is crucial for obtaining optimal enzymatic activity and the unique basic amino acid preference of APB *via* maintaining the appropriate catalytic pocket structure and thus for its function as a processing enzyme of peptide hormones and neurotransmitters.

1. Introduction

Aminopeptidases hydrolyze N-terminal amino acids of proteins or peptide substrates [1]. Among them, the M1 family of zinc aminopeptidases shares GXMEN and $HEXXH(X)_{18}E$ motifs essential for enzymatic activity. This family, which comprises 11 human enzymes, plays important roles in several pathophysiological processes including angiogenesis, cell cycle regulation, reproduction, memory retention, blood pressure regulation and antigen presentation to major histocompatibility complex class I molecules [2].

Aminopeptidase B (EC 3.4.11.6, APB) is a monomeric secretory protein first detected in several rat tissues which preferentially removes basic amino acids (Arg and Lys) from the N-terminus of several peptide and fluorogenic substrates [3]. Characterization of the enzymatic properties of APB showed that the hydrolytic activity of the enzyme was enhanced in the presence of physiological concentrations of chloride anions [4].

cDNA cloning of the rat APB revealed that the enzyme belongs to the M1 family and is closely related to leukotriene A_4 hydrolase (LTA4H), which converts LTA_4 to LTB_4 [5,6]. LTA4H contains both GXMEN and $HEXXH(X)_{18}E$ motifs and also has aminopeptidase activity [7]. Similarly, it was reported that human APB also shows hydrolytic activity toward LTA_4, suggesting that the enzyme plays a role in certain inflammatory processes; however, another group could not detect this activity [6,8].

Since APB shows preference for basic amino acids, this enzyme has been suggested to be involved in the proteolytic processing and maturation of peptide hormones and neurotransmitters [3,9]. APB has been reported to be involved in the generation of active peptides through cleavage of extended N-terminal Arg and Lys residues in intermediate propeptides produced by endopeptidases such as cathepsin L and N-arginine dibasic convertase (NRD)/nardilysin [9–11]. Moreover, APB co-localizes with cathepsin L in neuropeptide-containing secretary

Abbreviations: APB, aminopeptidase B; IC_{50}, half maximal (50%) inhibitory concentration; EC_{50}, half maximal (50%) effective concentration; ERAP, endoplasmic reticulum aminopeptidase; LTA4H, leukotriene A_4 hydrolase; MCA, 4-methylcoumaryl-7-amide; NRD, N-arginine dibasic convertase

* Corresponding author at: Faculty of Pharmaceutical Sciences, Teikyo Heisei University, 4-21-2 Nakano, Nakano, Tokyo 164-8530, Japan. Tel.: +81 3 5860 4251.
E-mail address: tsujimot@thu.ac.jp (M. Tsujimoto).

0304-4165/$ – see front matter © 2014 Elsevier B.V. All rights reserved.
http://dx.doi.org/10.1016/j.bbagen.2014.01.002

vesicles [9]. Given that the hydrolytic activity of APB toward Arg and Lys residues is essential for processing and maturation of hormones and neurotransmitters, it is important to elucidate the structural aspects underlying APB activity. In this context, Fukasawa et al. reported that replacement of Asp405 with Ala or Asn in rat APB caused a change of substrate specificity toward fluorogenic substrates [12].

Residues responsible for substrate specificity of M1 aminopeptidases have been identified. Here, Gln181 of human endoplasmic reticulum aminopeptidase 1 (ERAP1) was found to be a residue important for ERAP1 substrate specificity [13]. Analysis of the recently resolved ERAP1 crystal structure revealed that Gln181 of human ERAP1 occupies the S1 site of the enzyme [14,15]. Replacement of Gln181 with Asp demonstrated that the mutant enzyme has a preference for basic amino acids, suggesting that Asp in this position is important for basic amino acid preference. Moreover, ERAP2 shows a preference for basic amino acids and has an Asp residue in the corresponding site and substitution of this residue with Gln abrogated the basic amino acid preference of this enzyme [13,16]. However, the corresponding residue of human APB is a Gln, despite the observation that this enzyme has a preference for basic amino acids.

Site-directed mutagenesis is a useful approach to elucidate mechanisms of enzymatic activity [17–19]. Using this approach, two consensus motifs, HEXXH$(X)_{18}$E and GXMEN, were identified to be critical for the hydrolytic activities shared by the M1 family of aminopeptidases. Both His residues and the second Glu in the HEXXH$(X)_{18}$E motif function as zinc ligands and are essential for the catalytic activity of M1 aminopeptidases, whereas the first Glu residue polarizes a water molecule and promotes nucleophilic attack of the carbonyl carbon of the peptide bond, forming a tetrahedral intermediate. On the other hand, Glu and Asn in the GXMEN motif are important for exopeptidase specificity through interaction with the N-terminal amide of substrates [17,20,21]. Moreover, it was recently reported that the Gly in GXMEN contributed to enzymatic activity and substrate specificity of M1 aminopeptidases [22,23].

In this study, we have analyzed the role of human APB Gln169, which corresponds to Gln181 of ERAP1, by site-directed mutagenesis analysis. We found that Gln169 was required for the preferential cleavage of Arg- and Lys-MCA fluorogenic substrates, chloride anion sensitivity and the maximal enzymatic activity toward several peptide substrates with N-terminal basic amino acids. Our data suggest that Gln169 (together with Asp406) is important to maintain the basic amino acid preference of APB, which is essential for its function as a precursor processing enzyme of hormones and neurotransmitters.

2. Materials and methods

2.1. Molecular modeling of the human APB

The recently published X-ray crystallographic structure of the human LTA4H with the RSR substrate (PDB ID: 3B7S) was used as a template for modeling the catalytic site of the human APB using the SWISS-MODEL Internet server (http://swissmodel.expasy.org/). To optimize the structure, hydrogen atoms were added to the initial model and the protonation states were assigned using the Protonate-3D tool within the MOE2012.10 software package (Chemical Computing Group, Montreal, QC, Canada). Energy minimization was then carried out using the AMBER12:EHT forcefield. For docking calculations, the backbones of the model (APB and RSR) were fixed and side-chain conformations were then subjected to another refinement procedure, including several rounds of energy minimization (until convergence) using a Molecular Mechanics method. We also built models of Gln169Asn and Gln169Glu, as well as the wild-type. The structures were represented using the CueMol program (R. Ishitani, CueMol: Molecular Visualization Framework).

2.2. Site-directed mutagenesis

DNA sequences encoding mutant APBs were generated by the polymerase chain reaction (PCR) using the full-length human APB cDNA (RIKEN clone ID: IRAL002L13) as the template. PCRs were carried out in 0.2 mL microcentrifuge tubes with 30 μL reaction volumes and performed for 1 cycle at 95 °C for 4 min, followed by 20 cycles at 95 °C for 1 min, at 55 °C for 1 min, and at 68 °C for 18 min using Pyrobest DNA polymerase (Takara, Otsu, Japan). The sense primer A (5′-TAGAGGATCCATGGCGAGCGGCGAGCATT-3′), containing a *Bam*HI sequence for directional cloning and the initiation ATG codon (underlined), and antisense primers complementary to the desired sequences were used for the amplification of upstream fragments. Downstream fragments were amplified using mutagenic sense primers and primer B (5′-TGAGTCGACCTAACTGCCCTTGGGT-3′) containing the *Sal*I sequence.

The two products of these reactions were used as templates for the second round of PCR. Secondary PCR was carried out with primers A and B for 1 cycle at 95 °C for 4 min, followed by 20 cycles at 95 °C for 1 min, at 55 °C for 1 min, and at 68 °C for 18 min. The resultant products were inserted into the expression vector, pQE-30 vector (Qiagen, Valencia, CA, USA), using the TOPO-cloning system (Invitrogen, La Jolla, CA). The DNA sequences of the products were commercially confirmed (Operon Biotechnologies, Tokyo, Japan).

2.3. Expression and purification of the recombinant APB and the mutants

The resultant plasmids were transformed into the *Escherichia coli* JM109 strain to produce recombinant proteins. For the expression of the recombinant human APB or its mutants, bacteria were precultured until the OD_{600} reached 0.5–0.7. To induce synthesis of the recombinant proteins, isopropyl β-D-thiogalactopyranoside (IPTG) was added to the cultures to a final concentration of 0.2 mM. Cells were cultured overnight at 28 °C in 1 L of Luria–Bertani broth containing 100 μg/mL ampicillin.

To purify the recombinant proteins, bacteria were collected by centrifugation at 4000 ×*g* for 20 min and sonicated on ice five times for 30 s using a sonicator (Model 250D sonifier, Branson, Danbury, CT, USA). Soluble proteins were recovered after centrifugation at 10,000 ×*g*, and the supernatants were applied to a DEAE Toyopearl (Tosoh, Tokyo, Japan) column equilibrated in 25 mM Tris/HCl buffer (pH 7.5) and eluted with 25 mM Tris/HCl buffer (pH 7.5) containing 50 mM NaCl. The eluates were applied to a TALON (Clontech, Palo Alto, CA, USA) column and eluted with 150 mM imidazole. The active fractions were collected, concentrated and subjected to further characterization.

2.4. Measurement of APB aminopeptidase activity

The aminopeptidase activity of the recombinant human APB and its mutants was determined using fluorogenic substrates, aminoacyl-4-metheylcoumaryl-7-amides (aminoacyl-MCAs). The reaction mixtures contained various concentrations of amino-acyl-MCAs and the enzyme (0.1 μg/mL) in 50 μL of 20 mM Tris/HCl buffer (pH 7.4) with 150 mM NaCl, and were incubated at 37 °C for 15 min. The amount of released 7-amino-4-methylcoumarin was measured by spectrofluorophotometry (MTP-810Lab, Hitachi, Tokyo, Japan) at an excitation wavelength of 365 nm and an emission wavelength of 450 nm. The kinetic parameters were calculated from Lineweaver–Burk plots. The results are represented as K_m, k_{cat} and k_{cat}/K_m values. All measurements were performed in triplicate.

2.5. Effect of sodium chloride and inhibitors on APB aminopeptidase activity

To measure the effect of sodium chloride on aminopeptidase activity, the recombinant proteins (0.1 μg/mL) and 25 μM Arg-MCA were mixed

in 0.2 M borate buffer (pH 7.4) containing various concentrations of NaCl. After incubation, the amount of 7-amino-4-methylcoumarin released was measured as described above.

To evaluate the inhibitory effects of bestatin, arphamenine A and B, *o*-phenanthroline and $ZnCl_2$, recombinant proteins (0.1 μg/mL) were mixed with various concentrations of inhibitors in 50 μL of 20 mM Tris/HCl buffer (pH 7.4) containing 150 mM NaCl on ice for 5 min, then incubated with 25 μM Arg-MCA at 37 °C for 15 min, and the amount of released 7-amino-4-methylcoumarin was measured.

2.6. Cleavage of peptide hormones by APB and mutant enzymes

Peptide hormones (25 μM; Peptide Institute, Osaka, Japan) were incubated with the recombinant enzymes (4 μg/mL) at 37 °C for 4 h in 20 mM Tris/HCl buffer (pH 7.4) containing 150 mM NaCl. The reaction was terminated by the addition of 2.5% (v/v) formic acid. The reaction products were separated on a reversed-phase column, COSMOSIL $5C_{18}$-AR-300 (4.6 mm inner diameter × 250 mm, Nacalai Tesque, Kyoto, Japan) using an automated high-performance liquid chromatography system (LC-2010AHT; Shimadzu, Kyoto, Japan). Peptides generated from [Arg^0]-Met-enkephalin, kallidin, angiotensin III, Met-enkephalin and X-bradykinin were isocratically eluted at a flow rate of 0.5 mL/min with 19% acetonitrile containing 0.086% trifluoroacetic acid. Peptides generated from dynorphin A_{1-17} were loaded onto the column equilibrated in 10% (v/v) acetonitrile containing 0.088% (v/v) trifluoroacetic acid and eluted with a linear gradient of 10% (v/v) acetonitrile containing 0.088% (v/v) trifluoroacetic acid to 30% (v/v) acetonitrile containing 0.084% (v/v) trifluoroacetic acid in 20 min at a flow rate of 0.5 mL/min. Kinetic parameters were calculated from Lineweaver–Burk plots. All measurements were performed in triplicates.

2.7. Materials

Asp-, Gln-, Glu-, Ile-, Tyr-, Val- and S-benzyl-Cys-MCAs were purchased from Bachem AG (Bubendorf, Switzerland). Ala-, Arg-, Leu-, Lys-, Met- and Phe-MCAs were from the Peptide Institute (Osaka, Japan). Bestatin, arphamenine A, arphamenine B, *o*-phenanthroline, kallidin, angiotensin III and Met-enkephalin were also obtained from the Peptide Institute. [Arg^0]-Met-enkephalin was purchased from Phoenix Peptides (Belmont, CA, USA). X-bradykinins, where X is a desired N-terminal amino acid, were synthesized by the Research Resources Center of the RIKEN Brain Science Institute.

3. Results

3.1. Modeling of the catalytic pocket of APB

To identify amino acid residues responsible for the substrate specificity of APB, we first modeled the catalytic pocket of APB using LTA4H (3B7S) as a template. Phylogenetic analysis indicates that APB and LTA4H are the most closely related among the M1 family of aminopeptidases, representing a distinct subfamily [5,6,24]. Fig. 1A shows the molecular modeling of the human APB catalytic pocket containing a putative tripeptide substrate (RSR) that has an N-terminal Arg. Asp406 has been shown to contribute to the APB substrate specificity and is located near the N-terminal Arg of the substrate in the catalytic pocket. It is also apparent from the model that Gln169 is located near the N-terminal end of the substrate. Thus, our modeling suggests that both Gln169 and Asp406 occupy the S1 site of the enzyme and may influence its substrate specificity.

As shown in Fig. 1B, corresponding residues of APB Gln169 are conserved among M1 aminopeptidases (except APA, ERAP2 and APO). Gln169 corresponds to Asp221 of APA and Asp198 of ERAP2, which are responsible for the distinct substrate specificities of the respective enzymes [13,25,26]. Here, the Asp221 of APA contributes to the acidic amino acid preference *via* chelating calcium cations, whereas Asp198 of ERAP2 confers the enzyme with preference for basic amino acid substrates. In addition, when Gln181 of ERAP1 was substituted with Asp, the resultant mutant enzyme revealed a basic amino acid preference [13]. Thus, we focused on the potential enzymatic role of Gln169 of human APB, because the enzyme shows basic amino acid preference despite the presence of Gln at this position.

To elucidate the role of Gln169 in substrate specificity, the wild-type and mutant APB constructs were expressed in *E. coli* and purified to homogeneity. The Asp406Glu mutant was also expressed, purified and used as a reference.

3.2. Hydrolytic activities of the wild-type and mutant APBs toward fluorogenic substrates

Fig. 2 shows the enzymatic activities of the wild-type and mutant APBs toward various fluorogenic substrates. As shown previously [3], the wild-type APB preferentially cleaved the Arg-MCA substrate, followed by Lys-MCA, thereby revealing a clear preference for basic amino acids. As reported, the APB Asp406Glu mutant retains substantial enzymatic activity and cleaved Lys-MCA preferentially rather than Arg-MCA, indicating that Asp406 contributes to the enzymatic activity and substrate specificity of APB [12].

When the substrate specificity of Gln169Asn was examined, substantial hydrolytic activity was retained toward Arg-MCA; however, activity towards Lys-MCA was significantly reduced to almost the basal level. Table 1 shows the kinetic parameters of the wild-type enzyme and the Gln169Asn mutant using Arg-MCA and Lys-MCA as substrates. The catalytic efficiency (k_{cat}/K_m) of the wild-type enzyme toward Lys-MCA was about 4.5-fold less than the measure catalytic efficiency toward Arg-MCA. This observation was mainly due to an increase in K_m. On the other hand, while Gln169Asn APB retained substantial hydrolytic activity toward Arg-MCA (30% of the wild-type enzyme activity), it hydrolyzed Lys-MCA 17.3-fold less efficiently than Arg-MCA, because of an increase in K_m and a decrease in k_{cat}. We also generated other mutants (Gln169Asp, Gln169Glu, Gln169Lys, Gln169Arg and Gln169Ala) and found that these mutant enzymes, except Gln169Ala, showed negligible hydrolytic activities toward all the fluorogenic substrates tested (Fig. 2 and data not shown). As observed for the Gln169Asn mutant, the Gln169Ala mutant cleaved Arg-MCA but not Lys-MCA (data not shown). These results indicate that in addition to Asp406, Gln169 is important for the recognition of fluorogenic substrates by APB. While the side chain amino group of Gln169 appears to be essential for maximum activity of the enzyme, its side chain length also affected activity. It is conceivable that Gln169 broadens the basic amino acid substrate specificity of APB such that the protein recognizes Lys and Arg substrates, whereas the mutant enzymes (*i.e.*, Gln169Asn and Gln169Ala) preferentially target Arg residues, even though they retained substantial enzymatic activity.

3.3. Effects of aminopeptidase inhibitors on the enzymatic activities of the wild-type and mutant APBs

We next compared the effects of aminopeptidase inhibitors on hydrolytic activities of the wild-type and Gln169Asn mutant APBs toward the Arg-MCA substrate (Table 2). It is apparent that bestatin (Phe-Leu analog), arphamenine A (Arg-Phe analog) and arphamenine B (Arg-Tyr analog), which interact with the catalytic pocket of APB, all inhibited the wild-type enzyme much more efficiently than the mutant. Thus, it is likely that Gln169 is required to maintain the pocket structure in a suitable conformation for the wild-type enzyme to show preference towards both Arg and Lys substrates. On the other hand, IC_{50}s of *o*-phenanthroline and Zn^{2+} were similar for the enzymes, confirming that these inhibitors interfered with hydrolytic activities shared by the M1 family of aminopeptidases.

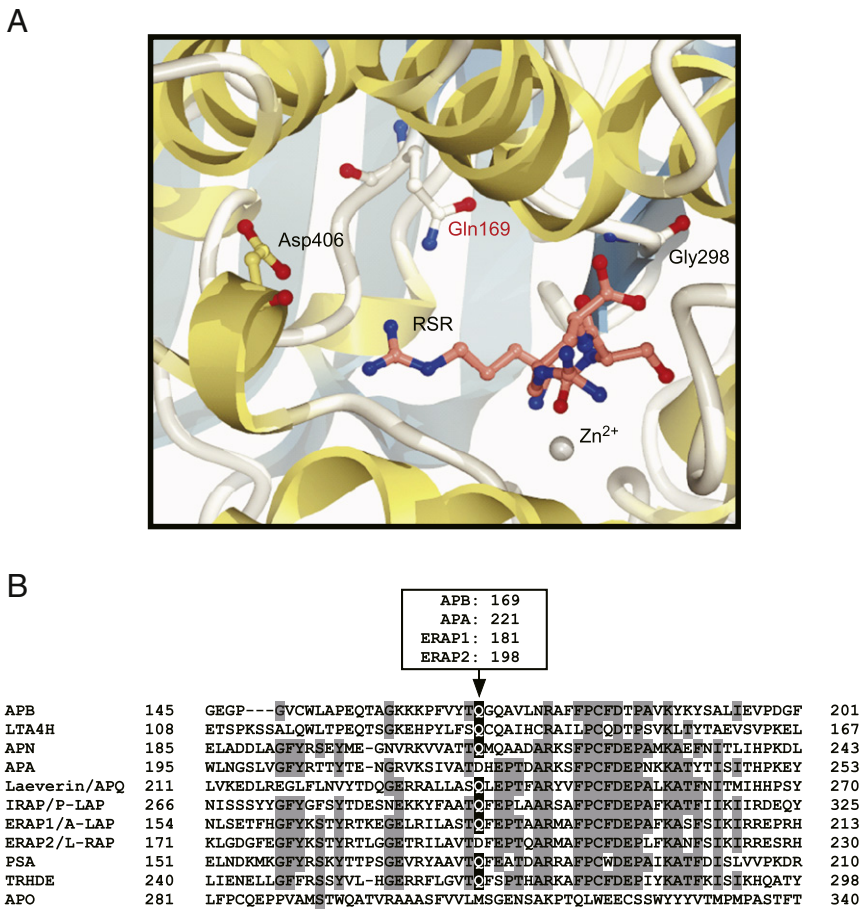

Fig. 1. Molecular modeling of the catalytic pocket of APB. A. Modeling of the catalytic site of APB bound with the putative substrate of RSR was performed using LTA4H as the template. Gln169 and Asp406 are shown as residues possibly interacting with the N-terminal Arg of the substrate. The location of Gly298 is also shown. B. Alignment around Gln169 of human APB with other human members of the M1 family of aminopeptidases. The amino acid sequence around Gln169 of human APB is compared with those of the other M1 aminopeptidases. The sequence data used for analysis were: APB (NM_020216); LTA4H (NM_000895); APN (NM_001150); APA (NM_001977); Laeverin/APQ (NM_173800); IRAP/P-LAP (NM_005575); ERAP1/A-LAP (NM_001040458); ERAP2/L-RAP (NM_022350); PSA (NM_006310); TRHDE (NM_013381); and APO (NM_032823). Gaps are inserted into the sequence to obtain optimal alignments. Residues corresponding to Gln169 of APB are highlighted in black. Residues conserved among the enzymes are shaded.

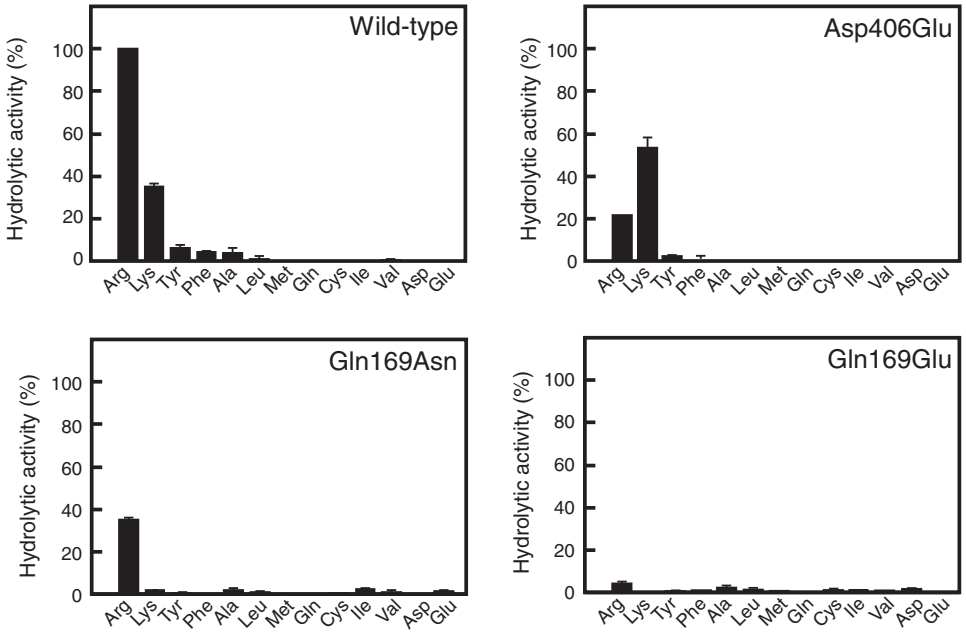

Fig. 2. Enzymatic activities of the wild-type and mutant APBs toward synthetic fluorogenic substrates. Purified enzymes (0.1 μg/mL) were incubated with 100 μM MCA substrates at 37 °C for 15 min. Hydrolytic activities are expressed relative to the wild-type enzyme activity (100%) toward Arg-MCA. Each bar shows mean ± S.D. ($n = 3$).

Table 1
Kinetic parameters of wild-type and Gln169Asn APBs toward Arg-MCA and Lys-MCA.

Substrate	APB	K_m (μM)	k_{cat} (s^{-1})	k_{cat}/K_m ($\mu M^{-1}\ s^{-1} \times 10^{-3}$)
Arg-MCA	Wild-type	53.3 ± 4.8	9.27 ± 0.93	175 ± 2
	Gln169Asn	77.4 ± 1.2	4.06 ± 0.34	52.4 ± 5.3
Lys-MCA	Wild-type	381 ± 9.7	14.9 ± 1.2	39.2 ± 3.6
	Gln169Asn	568 ± 11	1.95 ± 0.02	3.44 ± 0.01

Kinetic parameters were determined from Lineweaver-Burk plots. Reactions were performed at 37 °C for 15 min with 150 mM NaCl. The values are mean ± S.D. ($n = 3$).

3.4. Effect of NaCl on the enzymatic activities of the wild-type and mutant APBs

Chloride anions modulate the enzymatic activity of APB [4]. Fig. 3 shows the effect of NaCl on the enzymatic activities of the wild-type and Gln169Asn APBs. In the absence of NaCl, the hydrolytic activities of the wild-type and mutant enzymes toward Arg-MCA were barely detectable (not shown in the figure). As expected, at a physiological NaCl concentration (150 mM), an 8.5-fold increase in the hydrolytic activity of the wild-type enzyme toward Arg-MCA was observed when compared with the activities measured in the presence of 10 mM NaCl. On the other hand, when the Gln169Asn mutant was examined, NaCl-induced enhancement of the hydrolytic activity was attenuated and a 2.8-fold increase in the activity was observed at 150 mM NaCl. Based on the previous assumption that a chloride anion binding site(s) is located at or near the APB substrate binding site [22], these results suggest that the structural alterations around this ion binding site(s) are conferred by substitution of Gln with Asn in the mutant enzyme. The EC_{50} values showed different binding affinities towards the chloride anion (*i.e.*, 38.6 mM for the wild-type protein and 155 mM for the mutant enzyme), further suggesting the presence of different local structures around the anion binding site. Taken together, it is most plausible that the replacement of Gln169 induces significant structural modifications in the catalytic pocket of the enzyme that alter characteristics of the APB enzymatic activity.

3.5. Hydrolytic activities of the wild-type and mutant APBs toward peptide substrates

We next compared the cleavage of several peptide hormones by the wild-type and Gln169Asn mutant APBs. Fig. 4A shows the cleavage of [Arg^0]-Met-enkephalin (RYGGFM), a well-known substrate of APB [3], by the wild-type and Gln169Asn APBs. Generation and subsequent degradation of Met-enkephalin (YGGFM) by the wild-type enzyme was clearly observed and 67.2% of [Arg^0]-Met-enkephalin was degraded to Met-enkephalin (peak b) and de-[Tyr]-Met-enkephalin (GGFM, peak c) after 4 h incubation. On the other hand, only 7.6% of [Arg^0]-Met-enkephalin was converted to Met-enkephalin by Gln169Asn APB during the same period. Generation of de-[Tyr]-Met-enkephalin was not detected. A time course study, as demonstrated by a decrease in substrate levels, showed that the wild-type enzyme cleaved the substrate linearly up to at least 4 h. A significant decrease in the degradation of the substrate by the Gln169Asn mutant was observed during the same period.

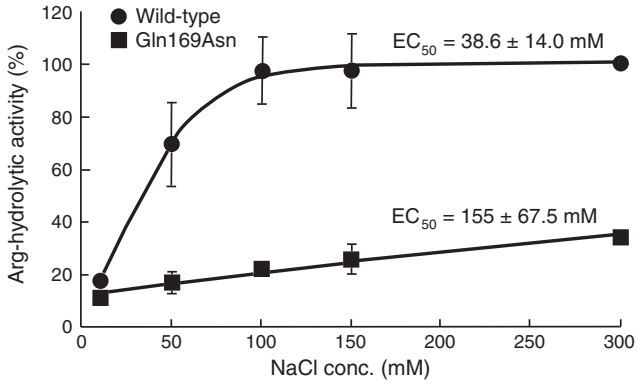

Fig. 3. Effect of the NaCl concentration on the enzymatic activities of the wild-type and mutant APBs. Hydrolytic activities are expressed relative to the wild-type enzyme activity (100%) in the presence of 300 mM NaCl. Each point represents the mean ± S.D. ($n = 3$).

When another substrate kallidin (Lys-bradykinin) (KRPPGFSPFR) [27] was tested, 74.9% of kallidin was converted to bradykinin by the wild-type enzyme within 4 h (Fig. 4B). On the other hand, the Gln169Asn mutant enzyme exhibited reduced activity and converted 33.8% of kallidin to bradykinin during the same period. A time course study showed a linear accumulation of bradykinin up to 4 h for the reaction with the wild-type enzyme (data not shown). However, the wild-type and Gln169Asn APBs did not cleave angiotensin III (RVYIHPF) (Fig. 4C), the fibronectin active fragment (RGDS) or substance P (RPKPQQFFGLM) (data not shown). These three substrates had an N-terminal Arg residue, indicating that not all peptides with N-terminal basic amino acids are good substrates. This observation is perhaps not surprising, because M1 aminopeptidases, like APB, cannot cleave N-terminal X-Pro sequences such as substance P and bradykinin [3,4,16,28].

We also tested the cleavage of several hormones without N-terminal Arg or Lys residues, including oxytocin (CYIQNCPLG-amide), neuronostatin 13 (LRQFLQKSLAAAA-amide), neurokinin A (HKTDSFVGLM-amide) and angiotensin (1–7) (DRVYIHP), and found that these hormones were not cleaved by either the wild-type or Gln169Asn APBs (data not shown).

Since the data shown in Fig. 4A imply that Met-enkephalin (the N-terminal amino acid is Tyr) is a substrate of the wild-type enzyme, we compared the direct cleavage of Met-enkephalin by the wild-type and Gln169Asn APBs (Fig. 5A). Met-enkephalin was cleaved by the wild-type enzyme with 16.3% of Met-enkephalin converted to de-[Tyr]-Met-enkephalin after 4 h incubation, whereas the mutant enzyme converted only 2.2% Met-enkephalin to de-[Tyr]-Met-enkephalin. A time course study indicated that although the accumulation level of cleaved peptide was low during the incubation time, linear accumulation was clearly observed up to 4 h. We also tested the APB-mediated cleavage of Leu-enkephalin (YGGFL), dynorphin A_{1-8} (YGGFLRRI), dynorphin A_{1-13} (YGGFLRRIRPKLK) and dynorphin A_{1-17} (YGGFLRRIRPKLKWDNQ), which share the N-terminal four residue sequence with Met-enkephalin, and found that these peptides were all cleaved by the enzyme. Interestingly, dynorphin A_{1-17} was cleaved ≈1.5-fold more efficiently than Met-enkephalin.

Table 2
IC_{50} values of the inhibitors toward wild-type and Gln169Asn APBs.

APB	Bestatin (nM)	Arphamenine A (nM)	Arphamenine B (nM)	*o*-Phenanthroline (μM)	$ZnCl_2$ (μM)
Wild-type	3.49 ± 0.56	3.73 ± 0.64	0.72 ± 0.06	77.0 ± 5.2	3.91 ± 0.36
Gln169Asn	289 ± 56	31.6 ± 5.5	1.55 ± 0.82	60.0 ± 6.9	5.92 ± 1.80

Purified enzymes (0.1 μg/mL) were incubated with 25 μM Arg-MCA substrates with various protease inhibitors in the presence of 150 mM NaCl. The hydrolytic activity toward Arg-MCA measured in the absence of an inhibitor was taken as 100%. The values representing IC_{50} values are means ± S.D. ($n = 3$).

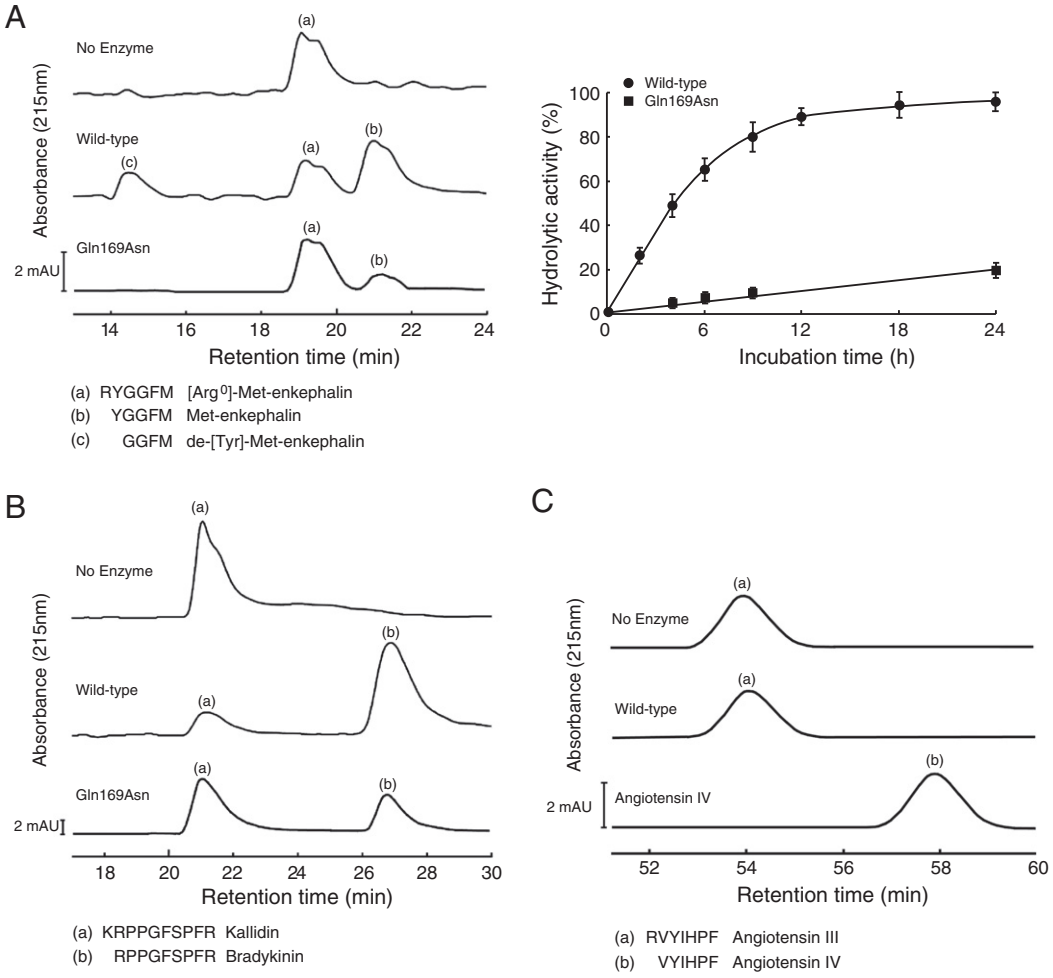

Fig. 4. Cleavage of [Arg^0]-Met-enkephalin, kallidin and angiotensin III by the wild-type and mutant APBs. [Arg^0]-Met-enkephalin (25 μM) (A) was incubated with the purified enzymes (4 μg/mL) at 37 °C for 4 h (left panel). The generated peptides were separated by HPLC. mAU: milli-absorbance units. Time course analyses of the wild-type and mutant APBs hydrolytic activities (right panel). [Arg^0]-Met-enkephalin (25 μM) was incubated with the purified enzymes (4 μg/mL) at 37 °C. The reaction was stopped at each time point, and the generated peptides were measured by HPLC. Each bar shows the mean ± S.D. ($n = 3$). Kallidin (25 μM) (B) or angiotensin III (25 μM) (C) was incubated with the purified enzymes (4 μg/mL) at 37 °C for 4 h, respectively. mAU: milli-absorbance units.

While the enzyme released 27.8% of the N-terminal Tyr of dynorphin A_{1-17} after 4 h incubation (Fig. 5B), Leu-enkephalin and the other dynorphin A peptides were cleaved with nearly the same efficiency as Met-enkephalin (data not shown), implying that peptide length is a determinant of the efficiency of APB-mediated substrate cleavage.

While it is known that substance P is not a substrate of APB [3,4], the finding that APB did not release the N-terminal Arg of angiotensin III was rather unexpected, because a previous study reported that angiotensin III was a substrate of rat APB [29]. Therefore we repeated the experiments and confirmed that angiotensin III was not cleaved by APB in the conditions we used or under the conditions used in the previous study.

To examine the interaction of peptides with APB, their binding to APB was assessed by a competition assay. Here, the hydrolysis of Arg-MCA was measured in the presence of each peptide [29]. Table 3 shows the effects of various peptides on the APB-mediated hydrolysis of Arg-MCA. While [Arg^0]-Met-enkephalin (100 μM) and kallidin (100 μM) showed ≈10% and ≈25% inhibition of the hydrolysis of Arg-MCA, respectively, angiotensin III (and the fibronectin active fragment) had negligible effect at the same concentration. On the other hand, substance P inhibited the hydrolysis of Arg-MCA (≈40% inhibition) more efficiently, suggesting that it bound to the enzyme more tightly than [Arg^0]-Met-enkephalin and kallidin. These results suggest that the interaction of angiotensin III with APB was not significant under the assay conditions used, reflecting its inability to be cleaved by the enzyme. In a previous study, a cell lysate was used and about a 10^4-fold higher IC_{50} value of arphamenine A was reported in comparison with that observed in our study [29]. The difference in the IC_{50} value previously reported and our reported value is presumably due to the presence of other contaminating aminopeptidases in the cell lysate, such as aminopeptidase N, ERAP1 and ERAP2, which may be responsible for the hydrolysis of angiotensin III [16,30,31]. Although it is documented that APB contributes to blood pressure regulation *via* inactivation of angiotensin III, a definitive confirmation can come only from a study that involves APB gene knockout animals [32,33].

Table 4 shows the kinetic parameters for the hydrolysis of the peptide substrates by the wild-type and Gln169Asn enzymes. The wild-type enzyme cleaved [Arg^0]-Met-enkephalin and kallidin with k_{cat}/K_m values of 0.173 $\mu M^{-1}\ s^{-1}$ and 0.156 $\mu M^{-1}\ s^{-1}$, respectively. On the other hand, the Gln169Asn mutant showed a 17.3-fold decrease in activity toward [Arg^0]-Met-enkephalin, because of an increase in K_m and a decrease in k_{cat}, indicating that the mutant lost a significant amount of activity toward one of the most preferable peptide substrates of the wild-type APB. Nonetheless, the mutant enzyme retained

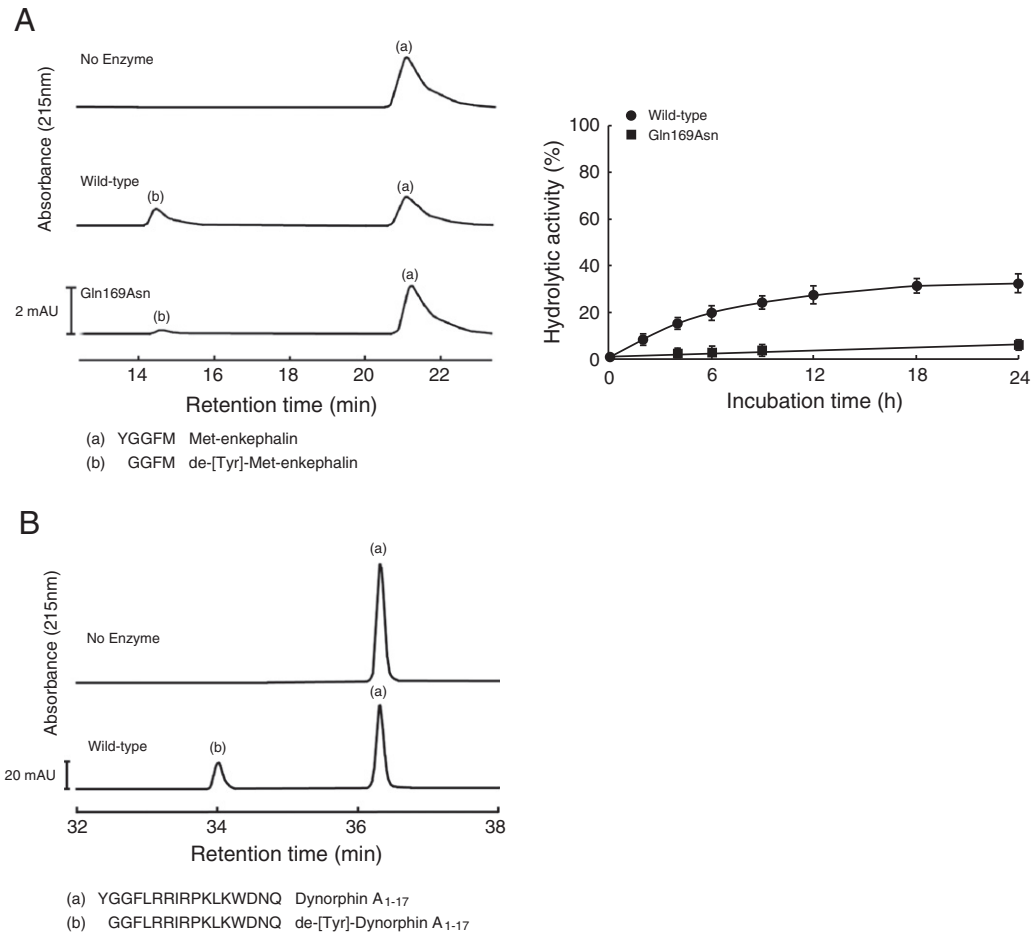

Fig. 5. Cleavage of Met-enkephalin and dynorphin A_{1-17} by the wild-type and mutant APBs. Met-enkephalin (25 μM) (A) was incubated with the purified enzymes (4 μg/mL) at 37 °C for 4 h (left panel). The generated peptides were separated by HPLC. mAU: milli-absorbance units. Time course analyses of the wild-type and mutant APBs hydrolytic activities (right panel). Met-enkephalin (25 μM) was incubated with the purified enzymes (4 μg/mL) at 37 °C. The reaction was stopped at each time point and the generated peptides were measured by HPLC. Each bar shows the mean ± S.D. (n=3). Dynorphin A_{1-17} (25 μM) (B) was incubated with the purified enzymes (4 μg/mL) at 37 °C for 4 h. The generated peptides were separated by HPLC. mAU: milli-absorbance units.

substantial hydrolytic activity toward the fluorogenic substrate Arg-MCA (30% of the wild-type enzyme activity). The mutant also showed 5.2-fold less activity toward kallidin, because of an increase in K_m and a slight decrease in k_{cat}, which is consistent with its hydrolytic activities toward Lys-MCA. Thus, hydrolytic potentials of the wild-type and mutant APBs toward peptide substrates do not exactly correspond to those toward fluorogenic substrates. Table 4 also shows that the wild-type enzyme cleaved Met-enkephalin more efficiently than the Gln169Asn mutant. Taken together, these results suggest that for peptide substrates, the presence of an N-terminal basic amino acid is not a prerequisite for APB enzymatic activity and peptides with N-terminal amino acids other than Arg and Lys (*i.e.*, Tyr) could be cleaved. However, because hydrolysis of Tyr-MCA was marginal, additional interactions between APB and the C-terminal region of Met-enkephalin may affect substrate recognition of APB towards the N-terminal Tyr residue.

To further elucidate the role of Gln169 in the enzymatic properties of APB, X-bradykinins were employed as substrates (Fig. 6). As was

Table 3
Inhibitory effects of various human peptide hormones on Arg-MCA hydrolytic activity of wild-type APB.

Peptide	Concentration (μM)	Arg-MCA hydrolysis (%)[a]
[Arg^0]-Met-enkephalin	10	96.8 ± 4.6
(RYGGFM)	100	89.9 ± 6.5
Kallidin	10	98.7 ± 6.7
(KRPPGFSPFR)	100	73.7 ± 3.8
Angiotensin III	10	104.0 ± 6.6
(RVYIHPF)	100	101.4 ± 3.5
Fibronectin active fragment	10	99.9 ± 8.6
(RGDS)	100	101.6 ± 3.9
Substance P	10	78.0 ± 4.1
(RPKPQQFFGLM)	100	63.8 ± 6.3

Wild-type APB (1 μg/mL) was preincubated with each peptide in 25 mM Tris/HCl buffer (pH 7.5) containing 150 mM NaCl on ice for 5 min, and the mixtures were incubated at 37 °C for 5 min after the addition of 25 μM Arg-MCA.
[a] The values are means ± S.D. (n = 3).

Table 4
Kinetic parameters of the wild-type and Gln169Asn APBs toward the peptide hormones.

Substrate	APB	K_m (μM)	k_{cat} (s^{-1})	k_{cat}/K_m ($\mu M^{-1}\ s^{-1} \times 10^{-3}$)
[Arg^0]-Met-enkephalin	Wild-type	21.0 ± 8.7	3.63 ± 0.42	173 ± 38
(RYGGFM)	Gln169Asn	111 ± 27	1.07 ± 0.24	10.4 ± 0.2
Kallidin	Wild-type	15.7 ± 4.0	2.35 ± 0.30	156 ± 28
(KRPPGFSPFR)	Gln169Asn	65.1 ± 8.4	1.99 ± 0.36	30.1 ± 2.3
Met-enkephalin	Wild-type	25.1 ± 5.2	0.47 ± 0.10	19 ± 0.50
(YGGFM)	Gln169Asn	360 ± 62	0.48 ± 0.09	1.0 ± 0.02

Kinetic parameters were determined from Lineweaver–Burk plots. Reactions were performed at 37 °C for 4 h with 150 mM NaCl. The values are mean ± S.D. (n = 3).

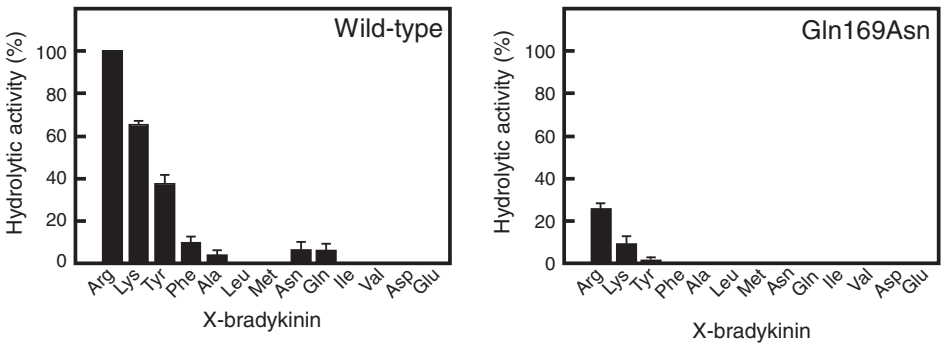

Fig. 6. Enzymatic activities of the wild-type and mutant APBs toward X-bradykinin. Purified enzymes (4 μg/mL) were incubated with 25 μM X-bradykinin substrates at 37 °C for 4 h. The generated bradykinin was separated by HPLC. The hydrolytic activities are expressed relative to the wild-type enzyme activity (100%) toward Arg-bradykinin. Each bar shows mean ± S.D. ($n = 3$).

observed for the fluorogenic substrates, the wild-type enzyme cleaved Arg-bradykinin most efficiently. In addition, as with Met-enkephalin, cleavage of Tyr-bradykinin was also remarkable. Phe-bradykinin was cleaved less efficiently, indicating that recognition of Tyr-bradykinin by APB arises from the presence of the hydroxyl group located on the benzene ring. These results imply that the interaction with the C-terminal region of the peptide substrate by the enzyme is also required to facilitate recognition of the N-terminal Tyr residue.

On the other hand, the Gln169Asn mutant showed reduced activity toward all substrates tested, further suggesting that the side chain length and presumably the amino group of Gln169 play important roles in the maintenance of maximal activity toward peptide substrates with N-terminal basic amino acids and possibly Tyr.

3.6. Role of Gln169 in the recognition of the N-terminal region of the substrate by APB

Fig. 7 shows a surface modeling of the catalytic pocket structure of the wild-type and mutant APBs occupied by RSR with special reference to the spatial relationship between residue Gln169 and the putative

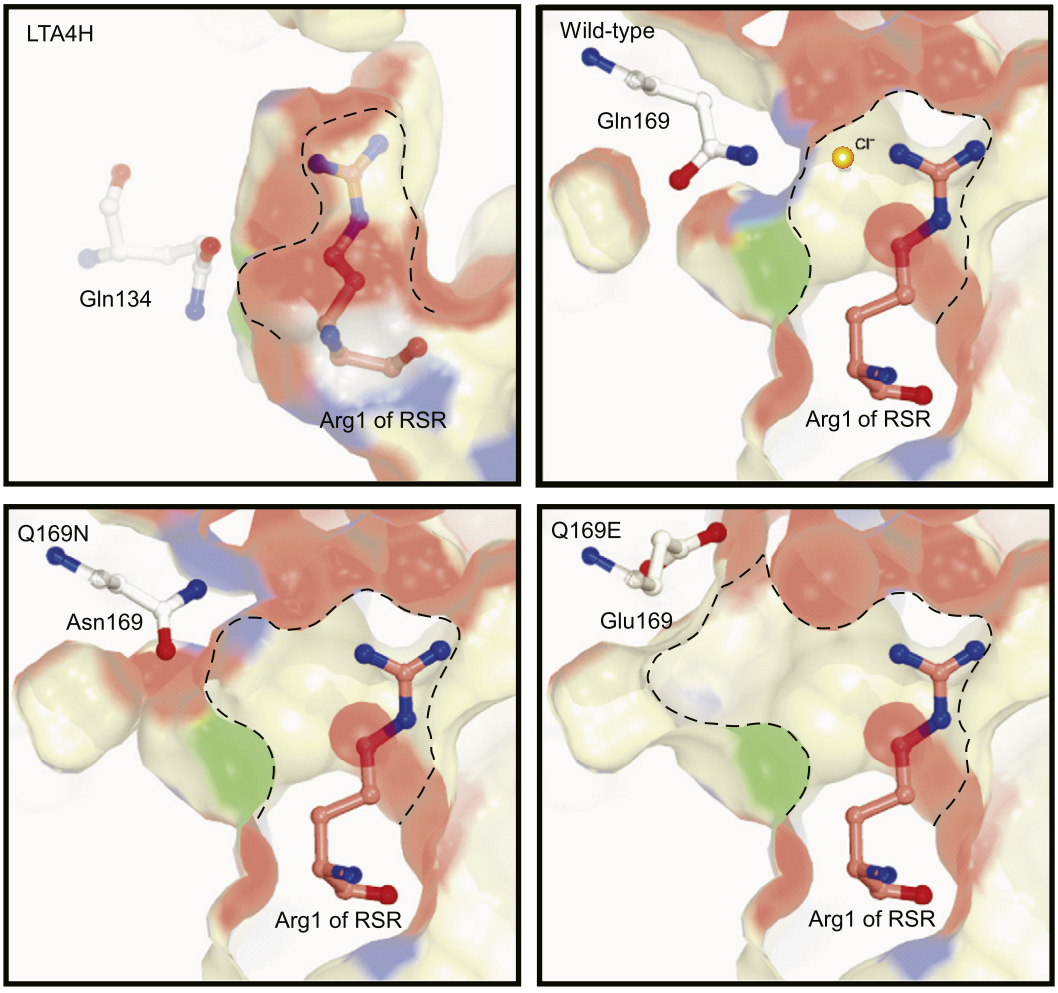

Fig. 7. Modeled structure of the S1 sites of the wild-type and mutant APBs. Frameworks of the S1 sites coupled with Arg1 of RSR are shown by electrostatic potential (red for negative and blue for positive). For comparison, the S1 site structure of LTA4H determined by X-ray crystallography is shown as a control.

substrate RSR. In the catalytic pocket of LTA4H, which is modeled as a reference, interaction of Arg1 of RSR with Gln134 is unlikely because of its inappropriate orientation relative to the amino group of Gln134. Chloride anion binding is also unlikely because there is no clear surface positive potential in the pocket. On the other hand, the catalytic pocket of the wild-type APB is wide enough to hold a chloride anion. The calculated distance between Arg1 of RSR and Gln169 (4.41−6.42 Å) suggests that although oriented properly, Arg1 of RSR cannot interact with Gln169 directly. Instead, the electric potential distribution provided by Gln169 suggests that the chloride anion can bridge the interaction between the two residues. When Gln169Asn and Gln169Glu were modeled, the catalytic pockets are also wide when compared with the catalytic pocket of LTA4H. However, substitution of Gln169 with Asn resulted in a loss of chloride anion sensitivity. It is possible that the chloride anion is not or only weakly retained in the pocket, because an appropriate surface positive potential in the pocket is missing. Alternatively, it is also possible that the retained chloride anion cannot interact with Asn169 of the mutant enzyme because of the shorter side chain. In the case of the Gln169Glu mutant, Glu169 is not correctly oriented to interact with either RSR or the chloride anion (if retained in the pocket). It is also plausible that Glu169 cannot provide an appropriate positive charge potential that is required for the retention of the chloride anion. Taken together, our molecular modeling suggests that interaction between Gln169 and the N-terminal amino acid of the substrate is bridged by a chloride anion, and is crucial for the enzymatic properties of the enzyme.

4. Discussion

In this study, the role of Gln169 in the enzymatic properties of human APB was elucidated. First, replacement of Gln169 with Asn changed the enzymatic activity of APB, resulting in either a total loss or substantial decrease in recognition of Lys- but not Arg-containing fluorogenic substrates. Second, Gln169 substitutions were found to attenuate chloride anion-dependent enhancement of the APB enzymatic activity. Finally, Gln169 is required for maximal activity toward peptide substrates, [Arg^0]-Met-enkephalin, kallidin and Met-enkephalin. Taken together, it is conclusive that Gln169 is critical for maintenance of APB optimal enzymatic activity and basic amino acid preference (especially for Lys) required for processing of prohormones and neurotransmitter precursors.

Substitution of Gln169 with Asn caused a significant reduction in the sensitivity toward chloride anions. It has been reported that a reduction in chloride anion sensitivity is observed when Gly298 of the GXMEN motif of rat APB is replaced with other amino acids such as Ser and Pro [22]. A close look at the catalytic pocket suggests that Gln169 is placed adjacent to Gly298 (Fig. 1). It is thus plausible that both amino acid residues participate in the coordination of the chloride anion in the catalytic pocket. Replacement of either Gln169 or Gly298 may cause an alternation of the local structure of the pocket that weakens anion binding. Changes of the inhibitor profile by substitution of Gln169 with Asn support the notion that Gln169 is important for maintaining the structure of the catalytic pocket for optimal catalytic activity.

It is remarkable that in spite of the presence of an N-terminal Arg residue, angiotensin III, the fibronectin active fragment and substance P were not hydrolyzed by the enzyme. Substance P is not cleaved by APB because of the presence of a Pro residue at the P1′ site [4,16]. In the case of angiotensin III and the fibronectin active fragment, it is also possible that the peptide-length and/or structure affects their recognition and processing by the enzyme [34,35]. In fact, although cleavage of Tyr-MCA by the wild-type enzyme was negligible, the N-terminal Tyr of Tyr-bradykinin was released rather efficiently, supporting the involvement of interactions between the C-terminal regions of the peptides and APB in defining substrate affinity. The cleavage pattern of dynorphin A peptides may reveal a peptide-length-dependent action of the enzyme. Different IC_{50} values shown by arphamenine A and B also support the notion that the site adjacent to the N-terminal amino acid of the peptide substrate plays a role in the substrate affinity of the enzyme.

This paper describes APB-mediated cleavage of N-terminal Tyr-containing Met-enkephalin and dynorphin A peptides for the first time. Although the k_{cat}/K_m value toward Met-enkephalin is ≈10-fold lower than that of [Arg^0]-Met-enkephalin, APB-mediated sequential processing of [Arg^0]-Met-enkephalin to de-[Tyr]-Met-enkephalin was clearly observed. Since deletion of the N-terminal Tyr residue inactivates these opioid hormones [36], it is interesting to speculate that while APB acts as a maturation enzyme of enkephalin processed from proenkephalin A/B through rapid liberation of the N-terminal Arg of the intermediate [Arg^0]-Met/Leu-enkephalin [37], it is also involved in the inactivation of hormones by mediating gradual release of an N-terminal Tyr residue. However, further research is necessary to verify whether Met-enkephalin can be a physiological substrate of the enzyme *in vivo*.

In the study of the substrate specificity of M1 aminopeptidases, we identified Asp221 of human APA as a critical residue [25]. We also found that the corresponding residue of the human ERAP1, Gln181, is critical for its substrate specificity [13]. In the case of wild-type ERAP2 and the Gln181Asp mutant ERAP1, both of which show basic amino acid preferences, the corresponding sites are occupied by Asp. We speculate that electrostatic interactions between this residue and the basic amino acid of the substrates are critical in defining the preference. However, the corresponding residue of human APB is Gln, and it was suggested that Asp406 contributed to the substrate specificity of the enzyme [12]. Our modeling of the catalytic pocket of the enzyme reveals that both Gln169 and Asp406 can interact with the side chain of the N-terminal Arg residue of the substrate. It is therefore conceivable that electrostatic interactions required for APB binding to basic amino acids are derived from Asp406, which causes stabilization of the enzyme-substrate complex, whereas Gln169 plays a role in the maintenance of the APB catalytic pocket conformation. Considering the data shown in Fig. 2, it is tempting to speculate that Gln169 contributes primarily to the recognition of N-terminal Lys residues, whereas Asp406 contributes to the recognition of N-terminal Arg residues. Taken together, these two residues may interact cooperatively with N-terminal amino acids of the substrate and thus create the unique substrate specificity observed for APB.

Fig. 8 shows a possible substrate recognition scheme of APB based on the present study. Gln169 interacts indirectly with the amino group of

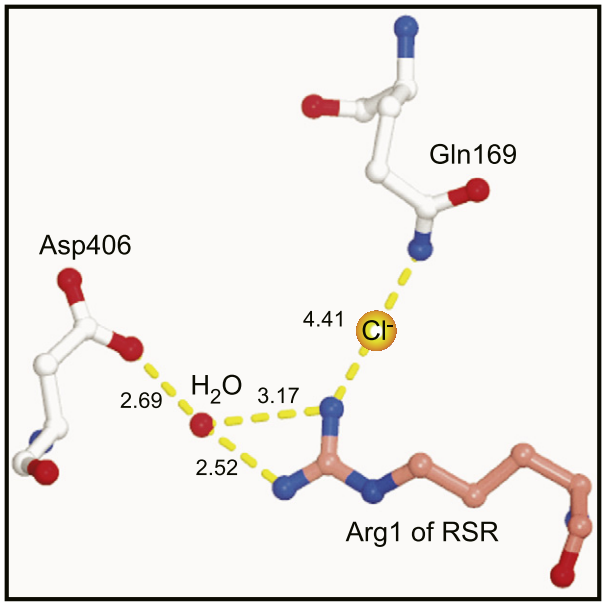

Fig. 8. Schematic representation of the recognition mechanism of APB towards the N-terminal Arg of a peptide substrate. Possible interactions between residues are shown by dotted lines with distances (Å).

the N-terminal Arg residue of a substrate peptide, and this interaction is mediated by a chloride anion. It was reported that chloride anions interact with side chains of basic amino acids when the distance between the two moieties is ideal [38,39]. In analogy with LTA4H [40], Asp406 may participate in the N-terminal Arg recognition *via* H_2O-bridged hydrogen bonds. However, it is possible that Gln169 interacts directly with another residue to form the appropriate structure of the catalytic pocket.

In this study, we have shown that Gln169 of the human APB is important in ensuring maximum enzymatic activity. This residue contributes, in concert with Asp406, to define the APB substrate preference for basic amino acids and thus to the biological function of APB in proteolytic processing of protein precursors. It is also plausible that in addition to the interaction with N-terminal amino acids of peptide substrates, a second interaction with the C-terminal region of the peptides is important for their cleavage by the enzyme. The high resolution structure of APB is required to confirm the molecular basis of the enzyme substrate specificity.

Acknowledgement

This work was supported in part by a Grant-in-aid from the Ministry of Education, Culture, Sports, Science and Technology of Japan.

References

[1] A. Taylor, Aminopeptidases: structure and function, FASEB J. 7 (1993) 290–298.
[2] M. Tsujimoto, A. Hattori, The oxytocinase subfamily of M1 aminopeptidases, Biochim. Biophys. Acta 1751 (2005) 9–18.
[3] S. Cadel, C. Piesse, V.-L. Pham, J. Pernier, C. Hanquez, C. Gouzy-Darmon, T. Foulon, Aminopeptidase B, in: N.D. Rawlings, G.S. Salvesen (Eds.), Handbook of Proteolytic Enzymes, 3rd edition, Academic Press, London, 2013, pp. 473–479.
[4] S. Cadel, A.R. Pierotti, T. Foulon, C. Creminon, N. Barre, D. Segretain, P. Cohen, Aminopeptidase-B in the rat testes: isolation, functional properties and cellular localization in seminiferous tubules, Mol. Cell. Endocrinol. 110 (1995) 149–160.
[5] K.M. Fukasawa, K. Fukasawa, M. Kanai, S. Fujii, M. Harada, Molecular cloning and expression of rat aminopeptidase B, J. Biol. Chem. 271 (1996) 30731–30735.
[6] S. Cadel, T. Foulon, A. Viron, A. Balogh, S. Midol-Monnet, N. Noel, P. Cohen, Aminopeptidase B from the rat testis is a bifunctional enzyme structurally related to leukotriene-A_4 hydrolase, Proc. Natl. Acad. Sci. U. S. A. 94 (1997) 2963–2968.
[7] M.M. Thunnissen, P. Nordhund, J.Z. Haeggstrom, Crystal structure of human leukotriene A_4 hydrolase, a bifunctional enzyme in inflammation, Nat. Struct. Biol. 8 (2001) 131–135.
[8] K.M. Fukasawa, K. Fukasawa, M. Harada, J. Hirose, T. Izumi, T. Shimizu, Aminopeptidase B is structurally related to leukotriene-A_4 hydrolase but is not a bifunctional enzyme with epoxide hydrolase activity, Biochem. J. 339 (1999) 497–502.
[9] S.-R. Hwang, A. O'Neill, S. Bark, T. Foulon, V. Hook, Secretary vesicle aminopeptidase B related to neuropeptide processing: molecular identification and subcellular localization to enkephalin-and NPY-containing chromaffin granules, J. Neurochem. 100 (2007) 1340–1350.
[10] G. Fontes, A.-D. Lajoix, F. Bergeron, S. Cadel, A. Prat, T. Foulon, R. Gross, S. Dalle, D. Le-Nguyen, F. Tribillac, D. Bataille, Miniglucagon (MG)-generating endopeptidase, which processes glucagon into MG, is composed of N-arginine dibasic convertase and aminopeptidase B, Endocrinology 146 (2005) 702–712.
[11] M. Beinfeld, L. Funkelstein, F. Foulon, S. Cadel, K. Kitagawa, T. Toneff, T. Reinheckel, C. Peters, V. Hook, Cathepsin L plays major role in cholecystokinin production in mouse brain cortex in pituitary AtT-20 cells: protease gene knockout and inhibitor studies, Peptides 30 (2009) 1882–1891.
[12] K.M. Fukasawa, J. Hirose, T. Hata, Y. Ono, Aspartic acid 405 contributes to the substrate specificity of aminopeptidase B, Biochemistry 45 (2006) 11425–11431.
[13] Y. Goto, H. Tanji, A. Hattori, M. Tsujimoto, Glutamine-181 is crucial in the enzymatic activity and substrate specificity of human endoplasmic-reticulum aminopeptidase-1, Biochem. J. 416 (2008) 109–116.
[14] T.T. Nguyen, S.-C. Chang, I. Evnouchidou, I.A. York, C. Zikos, K.L. Rock, A.L. Goldberg, E. Stratikos, L. Stern, Structural basis for antigenic peptide precursor processing by endoplasmic reticulum aminopeptidase ERAP1, Nat. Struct. Mol. Biol. 18 (2011) 604–613.
[15] G. Kochan, T. Krojer, D. Harvey, R. Fischer, L. Chen, M. Vollmar, F. von Delft, K.L. Kavanagh, M.A. Brown, P. Bowness, P. Wordsworth, B.M. Kessler, U. Oppermann, Crystal structures of the endoplasmic reticulum aminopeptidase-1 (ERAP1) reveal the molecular basis for N-terminal peptide trimming, Proc. Natl. Acad. Sci. U. S. A. 108 (2011) 7745–7750.
[16] T. Tanioka, A. Hattori, S. Masuda, Y. Nomura, H. Nakayama, S. Mizutani, M. Tsujimoto, Human leukocyte-derived arginine aminopeptidase: the third member of the oxytocinase subfamily of aminopeptidases, J. Biol. Chem. 278 (2003) 32275–32283.
[17] M. Tsujimoto, Y. Goto, M. Maruyama, A. Hattori, Biochemical and enzymatic properties of the M1 family of aminopeptidases involved in the regulation of blood pressure, Heart Fail. Rev. 13 (2008) 285–291.
[18] P.G. Lausten, S. Vang, T. Kristensen, Mutational analysis of the active site of human insulin-regulated aminopeptidase, Eur. J. Biochem. 268 (2001) 98–104.
[19] V.-L. Pharm, M.-S. Cadel, C. Gouzy-Darmon, C. Hanquez, M.C. Beinfeld, P. Nicolas, C. Etchebest, T. Foulon, Aminopeptidase B, a glucagon-processing enzyme: site directed mutagenesis of the Zn^{2+}-binding motif and molecular modeling, BMC Biochem. 8 (2007) 21.
[20] G. Vazeux, X. Iturrioz, P. Corvol, C. Llorens-Cortes, A glutamate residue contributes to the exopeptidase specificity in aminopeptidase A, Biochem. J. 334 (1998) 407–413.
[21] X. Iturrioz, R. Rozenfeld, A. Michaud, P. Corvol, C. Llorens-Cortes, Study of asparagine 353 in aminopeptidase A: characterization of novel motif (GXMEN) implicated in exopeptidase specificity of monozinc aminopeptidases, Biochemistry 40 (2001) 14440–14448.
[22] V.-L. Pham, C. Gouzy-Darmon, J. Pernier, C. Hanquez, V. Hook, M.C. Beinfeld, P. Nicolas, C. Etchebest, T. Foulon, S. Cadel, Mutation in the substrate-binding site of aminopeptidase B confers new enzymatic properties, Biochimie 93 (2011) 730–741.
[23] M. Maruyama, N. Arisaka, Y. Goto, Y. Ohsawa, H. Inoue, H. Fujiwara, A. Hattori, M. Tsujimoto, Histidine 379 of human laeverin/aminopeptidase Q, a nonconserved residue within the exopeptidase motif, defines its distinctive enzymatic properties, J. Biol. Chem. 284 (2009) 34692–34702.
[24] A. Hattori, K. Matsumoto, S. Mizutani, M. Tsujimoto, Genomic organization of the human adipocyte-derived leucine aminopeptidase gene and its relationship to the placental leucine aminopeptidase/oxytocinase gene, J. Biochem. 130 (2001) 235–241.
[25] Y. Goto, A. Hattori, S. Mizutani, M. Tsujimoto, Aspartic acid 221 is critical in the calcium-induced modulation of enzymatic activity of human aminopeptidase A, J. Biol. Chem. 282 (2007) 37074–37081.
[26] Y. Yang, C. Liu, L. Fang, Structural insights into central hypertension regulation by human aminopeptidase A, J. Biol. Chem. 288 (2013) 25638–25645.
[27] V.K. Hopsu, K.K. Makinen, Formation of bradykinin from kallidin-10 by aminopeptidase B, Nature 212 (1966) 1271–1272.
[28] A. Hattori, M. Maruyama, H. Fujiwara, M. Tsujimoto, Aminopeptidase Q/Laeverin, in: N.D. Rawlings, G.S. Salvesen (Eds.), Handbook of Proteolytic Enzymes, 3rd edition, Academic Press, London, 2013, pp. 442–444.
[29] V.V. Petrov, R.H. Fagard, P.J. Lijnen, Arginine-aminopeptidase in rat cardiac fibroblastic cells participates in angiotensin peptide turnover, Cardiovasc. Res. 61 (2004) 724–735.
[30] A. Hattori, K. Kitatani, H. Matsumoto, S. Miyazawa, T. Rogi, N. Tsuruoka, S. Mizutani, Y. Natori, M. Tsujimoto, Characterization of recombinant human adipocyte-derived leucine aminopeptidase expressed in Chinese hamster ovary cells, J. Biochem. 128 (2000) 755–762.
[31] R.C. Speth, V.T. Karamyan, The significance of brain aminopeptidases in the regulation of the actions of angiotensin peptides in the brain, Heart Fail. Rev. 13 (2008) 299–309.
[32] I. Banegas, I. Prieto, F. Vives, F. Alba, M. de Gasparo, A.B. Segarra, F. Hermoso, R. Durán, M. Ramírez, Brain aminopeptidases and hypertension, J. Renin-Angiotensin-Aldosterone Syst. 7 (2006) 129–134.
[33] M. Ramírez, I. Prieto, F. Alba, F. Vives, I. Banegas, M. de Gasparo, Role of central and peripheral aminopeptidases activities in the control of blood pressure: a working hypothesis, Heart Fail. Rev. 13 (2008) 339–353.
[34] S.C. Chan, F. Momburg, N. Bhutani, A.L. Goldberg, The ER aminopeptidase, ERAP1, trims precursors to lengths of MHC class I peptides by a "molecular ruler" mechanism, Proc. Natl. Acad. Sci. U. S. A. 102 (2005) 17107–17112.
[35] I. Evnouchidou, F. Momburg, A. Papakryriakou, A. Chroni, L. Leondiadis, S.C. Chang, A.L. Goldberg, E. Stratikos, The internal sequence of the peptide-substrate determines its N-terminus trimming by ERAP1, PLoS ONE 3 (2008) e3658.
[36] I. Berezniuk, L.D. Fricker, Endogenous opioids, in: G.W. Pasternak (Ed.), The Opiate Receptors, 2nd edition, Springer, New York, 2011, pp. 93–120.
[37] T.J. Krieger, L. Mende-Mueller, V.Y. Hook, Prohormone thiol protease and enkephalin precursor processing: cleavage at dibasic and monobasic sites, J. Neurochem. 59 (1992) 26–31.
[38] C.-H. Tai, P. Burkhard, D. Gani, T. Jenn, C. Johnson, P.F. Cook, Characterization of the allosteric anion-binding site of o-acetylserine sulfhydrylase, Biochemistry 40 (2001) 7446–7452.
[39] S. Duquerroy, A. Vigouroux, P.J.M. Rottier, F.A. Ray, B.J. Bosch, Central ions and lateral asparagine/glutamine zippers stabilize the post-fusion hairpin conformation in the SARS coronavirus spike glycoprotein, Virology 335 (2005) 276–285.
[40] F. Tholander, A. Muroya, B.P. Roques, M.C. Foumié-Zaluski, M.M. Thunnissen, J.Z. Haeggström, Structure-based dissection of the active site chemistry of leukotriene A4 hydrolase: implications for M1 aminopeptidases and inhibitor design, Chem. Biol. 15 (2008) 920–929.